HHS Public Access

Author manuscript

Nature. Author manuscript; available in PMC 2015 October 05.

Published in final edited form as:

Nature. ; 484(7395): 546–549. doi:10.1038/nature10999.

Crowding induces live cell extrusion to maintain homeostatic cell numbers in epithelia

George T. Eisenhoffer[1,*], **Patrick D. Loftus**[1,*], **Masaaki Yoshigi**[2], **Hideo Otsuna**[3], **Chi-Bin Chien**[3], **Paul A. Morcos**[4], and **Jody Rosenblatt**[1]

[1]Department of Oncological Sciences, Huntsman Cancer Institute, University of Utah, 2000 Circle of Hope Drive, Salt Lake City, UT 84132

[2]Department of Pediatrics, University of Utah, 295 Chipeta Way RM 2S010, Salt Lake City, UT 84108

[3]Department of Neurobiology and Anatomy, University of Utah, 401 MREB, 20N 1900E, Salt Lake City, UT 84132

[4]Gene Tools, LLC, 1001 Summerton Way, Philmath, OR 97370

For an epithelium to provide a protective barrier, it must maintain homeostatic cell numbers by matching the number of dividing and dying cells. While compensatory cell division can be triggered by dying cells[1–3], how cell death might relieve overcrowding due to proliferation is not known. When we trigger apoptosis in epithelia, dying cells are extruded to preserve a functional barrier[4]. To extrude, cells destined to die signal surrounding epithelial cells to contract an actomyosin ring that squeezes the dying cell out [4–6]. However, it is not clear what drives cell death during normal homeostasis. We show that overcrowding, due to proliferation and migration, induces extrusion of live cells to control epithelial cell numbers. Live cell extrusion occurs at sites where highest crowding occurs *in vivo* and can be induced by experimentally overcrowding monolayers *in vitro*. Like apoptotic cell extrusion, live cell extrusion resulting from overcrowding also requires Sphingosine 1-Phosphate (S1P) signalling and ROCK-dependent myosin contraction but is distinguished by signalling through stretch-activated channels. Moreover, disruption of a stretch-activated channel, Piezo1, in zebrafish prevents extrusion and leads to the formation of epithelial cell masses. Our findings reveal that during homeostatic turnover, growth and division of epithelial cells on a confined substratum causes overcrowding that leads to their extrusion and consequent death due to loss of survival factors. These results suggest that live

Correspondence and requests for materials should be addressed to: J.R. (jody.rosenblatt@hci.utah.edu) or M.Y. for inquiries on the stretching device.

*These authors contributed equally to this work

Author contributions. G.T.E. and P.D.L. both contributed to the study design and performed all the experiments. M.Y. designed the stretching apparatus and consulted in the study design. J.R. found preliminary results of live cell extrusion *in vivo* and contributed to the design of the study. G.T.E., J.R. and P.D.L. analysed the data and wrote the paper. P.M. designed the photo-cleavable morpholinos, and H.O. and C.B.C. provided zebrafish with epidermal Kaede expression. All authors discussed the results and commented on the manuscript.

The authors declare no competing interests.

cell extrusion could be a tumour suppressive mechanism that prevents the accumulation of excess epithelial cells.

To examine how cells are eliminated during homeostasis, we immunostained human colon tissues, developing zebrafish epidermis, and cultured Madin-Darby Canine Kidney (MDCK) epithelial cells for active-caspase-3 to identify apoptotic cells and actin and DNA to highlight cell borders and extrusion[4, 6]. Surprisingly, we found predominantly caspase-negative cells extrude from the surfaces of colon epithelia (80%, n=46 extruding cells), from zebrafish epidermis (88%, n=160 extruding cells in 3 experiments), and from overgrown monolayers in culture (67%, n=300 extruding cells in 3 experiments; Fig. 1 a,b,d,e,g,h). By contrast, extrusions resulting from inducing apoptosis in zebrafish with G418 or cultured monolayers with ultraviolet-C (UV-C) were almost exclusively caspase-3 positive[6]. These findings suggest that during homeostasis and development, live rather than dead cells are eliminated by extrusion. Similar live cell extrusions have been observed during mammary gland involution[7]. Because these non-apoptotic *in vivo* extrusions looked identical to apoptotic extrusion, we hypothesized that the extrusion pathway operates in two diverging manners: one to maintain homeostatic cell numbers in epithelia and the other to remove apoptotic/damaged cells.

When quantifying extrusion in both adult human colon and developing zebrafish epidermis, we noticed that extrusions occurred predominantly at the fin edges and colon surfaces, where cell densities were highest (1.7- and 1.8-fold higher than fin center or crypt side (Supplementary Fig. 1a&b), respectively, indicated by yellow cells in Fig. 1c,f). Extrusion zones were also more curved *in vivo*, yet, because they occurred most frequently in regions with higher cell density (1.8 fold) compared to proliferative regions in flat cell culture monolayers (Fig. 1i and Supplementary Fig. 1c), we decided to experimentally test if overcrowding strain could induce cells to extrude.

To simulate overcrowding observed *in vivo,* we grew MDCK cells to confluence on a silicone membrane stretched to 28% of its original length and then released it from stretch (Fig. 2a). Within 30 minutes after release, the number of cells per 100μm^2 increased 1.3-fold, from 112 ±5 to 144 ±4 (Fig. 2b–f). ZO-1 and β-catenin staining confirmed that tight and adherens junctions were still intact and that the average cell diameter had decreased by 30 minutes post-crowding (Fig. 2g–i and Supplementary Fig. 2). Moreover, crowded monolayers maintained adhesion to Cy-5-labeled fibronectin coated membranes (Fig. 2j). By 6 hours, the number of cells per field equilibrated to pre-release levels (110 ±10 cells/100μm^2, see Fig. 2e–f), indicating that MDCK epithelia eliminate cells to achieve homeostatic cell numbers.

Immunostaining for actin and active-caspase-3 showed that overcrowding induced predominantly non-apoptotic extrusion, similar to levels during homeostasis (Fig. 3a). Filming crowded MDCK monolayers expressing Lifeact-GFP[8] to highlight F-actin or the active-caspase-3 indicator NucView™ confirmed that live cells are extruded by contracting actin rings (Supplementary Movie 1 and Supplementary Fig. 4). The numbers of live extruding cells eventually decreased by 6 hours post-overcrowding concordantly with the

decrease in cell densities. The percentage of non-apoptotic extrusion also correlated to the percentage of crowding (Supplementary Fig. 3).

To determine whether live cell extrusions required the same factors that control apoptotic cell extrusion, we blocked signals required for extrusion during experimental overcrowding. We previously identified sphingosine-1-phosphate (S1P) as the signal apoptotic cells produce to activate the S1P receptor 2 ($S1P_2$), which triggers Rho-mediated contraction to squeeze the dying cells out[5]. Inhibiting Rho Kinase (ROCK) or S1P signalling dramatically decreased the percentages of both non-apoptotic and apoptotic cell extrusions (Fig. 3b). Although it was not possible to score non-apoptotic cells blocked from extrusion, as they look like any other cells within the monolayer, the significant decreases in percentages of non-apoptotic extrusion indicated that live cell extrusion, like apoptotic extrusion, requires S1P signalling through ROCK-mediated actomyosin contraction.

To assess the fate of overcrowding-induced extruded cells, we analysed their viability using flow cytometry and their ability to survive and proliferate by plating them on new substrata. After collecting extruded cells from the medium two hours post-crowding, 45.3 ± 2.1% were alive, whereas only 21.3 ± 2.7% were alive after UV-induced apoptotic extrusion (Fig. 3c and Supplementary Fig. 5a). Overcrowding and homeostatically extruded cells were able to proliferate into confluent monolayers, whereas those collected from apoptosis-induced extrusion did not (Fig. 3d). If, however, cells extruded from homeostatic or post-crowded monolayers were collected after 24 hours, most cells died instead of proliferating after replating (Supplementary Fig. 5b), suggesting that extruded cells typically die unless a new substratum is provided. Presumably, during homeostasis *in vivo* most extruded cells die from anoikis, apoptosis due to loss of survival signals from engagement with the underlying matrix[9–11].

We next investigated what signals trigger live cell extrusion during homeostasis or overcrowding. We previously found that over-expression of Bcl-2 inhibits both apoptosis and extrusion in response to apoptotic stimuli ([12] and Fig. 3f), however, Bcl-2 overexpression did not block live cell extrusion during homeostasis or following overcrowding (Figs. 3e, g). To investigate signals that might regulate live cell extrusion after overcrowding, we tested two candidates that are activated by cell stress: the c-terminal Jun Kinase (JNK)[13] and stretch-activated channels[14, 15]. JNK II inhibitor blocked apoptotic extrusion in response to UV-C but not live cell extrusion following overcrowding or homeostatic cell turnover (Figs. 3e–g). In contrast, we found that inhibiting stretch-activated ion channels with gadolinium (Gd^{3+})[16, 17] significantly reduced the percentage of both apoptotic and non-apoptotic extrusion events following overcrowding or during epithelial homeostasis, yet had no effect on apoptotic cell extrusion in response to UV (Fig. 3e–g). When cell extrusion is blocked by Gd^{3+}, the number of cells per 100 μm^2 remains high at 2 hours post-crowding (167 +/−12) compared to control crowded cells (112 +/−5), demonstrating that extrusion relieves overcrowded cell densities. Thus, while Bcl-2 and JNK control apoptosis-induced extrusion, stretch-activated signalling controls live cell extrusion during homeostasis that is induced by overcrowding, presumably upstream of S1P signalling (Fig. 4l).

If stretch-activated signalling controls extrusion-mediated homeostatic cell turnover, blocking this pathway *in vivo* should lead to accumulation of excess epithelial cells. By immunostaining and filming the epidermis of developing zebrafish with *Tg(cldnb:lynGFP)*[18], we found that cells proliferate at 37 hours post fertilization (hpf) and migrate to the fin edges between 48–59 hpf where they extrude at 60 hpf (Fig. 4a, c–e, Supplementary Fig. 6, and Movie 2). Treating 48 hpf zebrafish with Gd^{3+} blocked homeostatic cell extrusion and resulted in epidermal cell mass formation at the fin edges, the number of which was dependent on Gd^{3+} concentration (Fig. 4b, f–h, Supplementary Fig. 7 and Movie 3). Live imaging of Gd^{3+}-treated *Tg(cldnb:lynGFP)* zebrafish revealed that the cell masses formed at zones of convergence, where cells failed to extrude (Fig. 4h and Movie 4).

By knocking down candidate stretch-activated channels in zebrafish with morpholinos, we found that live cell extrusion requires the channel Piezo1[14]. To prevent developmental defects from early knockdown (Supplemental Fig. 8a&b), we used a photo-cleavable morpholino (photo-MO) to knockdown Piezo1 at 30 hpf (Supplemental Fig. 8c&d) [19]. By 60 hpf, Piezo1 morphants, like Gd^{3+}-treated fish could not extrude cells and developed epidermal masses at the fin edges and other sites of tissue strain (Figs. 4b, i–k and Supplementary Figs. 9&10), indicating that Piezo1 regulates extrusion to maintain homeostatic epithelial cell numbers *in vivo*.

As extrusion appears to control cell numbers during homeostasis, we predict that alterations in extrusion could lead to various epithelial pathologies. Aberrant signalling or tensions that block extrusion could lead to formation of cell masses, as those produced in zebrafish when stretch-activated channels are disrupted. Furthermore, these cell masses may set the stage for tumourigenesis by allowing retention of oncogenic or defective cells. In support of this, we found increased cell densities and no clearly identified extrusions in colon polyp sections compared to control sections (Supplementary Fig. 11). Conversely, hyper-contraction of bronchial epithelia following bronchoconstriction in asthmatics could lead to excessive extrusion and characteristic epithelial denuding. The resulting poor barrier could lead to increased inflammation and infection seen in asthmatics[20–22]. While mathematical models have suggested that mechanical forces could control tissue homeostasis[23], our results show that cell division and migration within epithelia cause overcrowding strain, which induces live cells to extrude and later die. Thus, homeostatic live cell extrusion provides the previously missing link between proliferation and epithelial cell death (Fig. 1c,f,i).

Materials and Methods Summary

All cell culture, cell staining, UV irradiation, and imaging were done using MDCK cells, as previously described[6]. Cells were treated with 10μM SKI-II (Calbiochem), 10μM JTE-013 (Tocris Bioscience), 10 μM SP600125, 10μM Gd^{3+}, (both Sigma-Aldrich), or 1% DMSO as a control. Flow cytometry was done use a Beckman-Dickinson FACScan after treating cells with 1μg/250μL of propidium iodide (Sigma-Aldrich). The Huntsman Cancer Institute Tissue Resource and Applications Core provided human colon sections. Developing wild-type AB zebrafish were treated with 10mM Gd^{3+} at 28.5°C until 60hpf, and immunostained according to[6] or filmed with a Nikon spinning disc confocal microscope using Andor

software. For the photo-MO experiments, the translation blocking antisense morpholino was mixed at 1:1 molar ratio with a 25bp sense photo-morpholino and injected into 1–2 cell stage wild-type AB or *Et(Gal4-VP16)^{zc1044a};Tg(UAS-E1b:Kaede)^{s1999t}* zebrafish embryos. At 28-32hpf, embryos were exposed to 350nm light for 20 seconds to release the caging sense-morpholino, then fixed and immunostained at 60 hpf.

Supplementary Methods

Cell Culture and Overcrowding Assays

Madin-Darby Canine Kidney (MDCK II) cells were grown as described[6]. A custom-design Teflon chamber (left) was fabricated to culture cells on flexible silicone membranes in stretched states (2×2 cm, 0.5 mm thickness)[24, 25]. Prior to cell seeding, 2×2 cm silicone membranes were stretched and coated with 5μg/mL fibronectin (BD Biosciences) at 4°C for 24 hrs. To stretch membranes with our device, one edge of the silicone membrane was clamped in place, while the other side was clamped to a movable shaft, which moves through a Teflon chamber with a sealing gasket. The movable shaft was pulled out to lengths representing 11%, 22% and 28% strain. 750,000 cells/ml were plated onto the 2×2 cm silicone matrices in a stretched state in the device or in a culture dish (for non-stretched controls) and grown to confluence, then released from their stretched states, thereby crowding cells in monolayer. Epithelial monolayers were fixed and stained or filmed using a Nikon 90i wide-field fluorescence microscope. Bcl-2 over-expressing cell lines are described in[12].

Drug and UV Assays

Confluent MDCK monolayers on silicone membranes were pre-treated with SP600125 JNK II inhibitor at 10, 50, and 100 μM or 10, 50, and 100 μM Gadolinium III Chloride (Gd^{3+}) for 30 minutes at 37°C. Apoptosis was induced by exposing monolayers to 1,200 μJ/cm^2 UV^{254} irradiation in a UV series II (Spectroline). Cells were fixed and stained from 1–6 hrs post-UV treatment depending on the experiment. The minimal drug concentrations (10 μM) established in the UV-induced extrusion assay were used in the overcrowding and homeostatic assays. For testing extrusion following overcrowding, chambers were pretreated with 10 μM JTE-013 (Tocris Bioscience), 10 μM SKI II (Calbiochem) or 10μM Y-27632 (Tocris) for 30 minutes prior to overcrowding up to 2 hours post-crowding.

Cell Immunostaining

Fixation and staining of MDCK II cells for actin, DNA, active-caspase 3, ZO-1, and β-catenin was carried out as previously described in[6]. Fibronectin was labeled with an Amersham Cy5 Ab Labeling Kit (GE Healthcare).

Live Cell Imaging

Standard MDCK cells or Lifact-GFP[8] expressing MDCK cells were grown to confluent monolayers and imaged on a Nikon 90i wide field fluorescent microscope with the stage kept at 37°C. For the Nucview experiments, cells were incubated with the activated caspase-3 indicator Nucview at 1:200 for 30 minutes prior to imaging.

Colon Sections

Human colon tissue samples were fixed, imbedded in paraffin, and cut into 10 μm sections by the Huntsman Cancer Institute Tissue Resource and Applications Core. The sections were deparaffinised and rehydrated by incubating in Citrus Clearing Solvent (CCS-Richard Allen Scientific), 100%, 95%, 80%, 70% ethanol, and PBS. Antigens were retrieved by heating the slides in 10 mM Sodium Citrate at 95°C for 20 minutes, then rinsed 3 times with PBS, blocked with 5% BSA/0.5% Tween-20 in PBS for 24 hours, and incubated overnight with active-caspase 3 antibody, rinsed 5 times with PBS, incubated in Alexa^{488}-anti- rabbit antibody, 1μg/ml Hoechst, and Alexa^{568}-anti-actin antibody for 2 hours, rinsed 3 times in PBS, and mounted in Prolong Gold (Invitrogen).

Microscopy

Images were captured on a CTR6000 microscope (Leica) with a 63x oil lens using a Micromax charge-coupled device camera (Roper Scientific) or on a Nikon Eclipse TE300 inverted microscope converted for spinning disc confocal microscopy (Andor Technologies) using a 20x or 60X plan fluor 0.95 oil lens with an electron-multiplied cooled CCD camera 1000 × 1000, 8 × 8 mm^2 driven by the IQ software (Andor Technologies). Image J was used to stack 8–10 consecutive 1μm confocal sections into Z series, which were then colour-combined and reconstructed into a 3D image using Metamorph (GE Healthcare). IP Lab 4.0.8 s and Image-J software were used to analyse percentages of apoptosis and extrusion. For quantification of extrusion in tissue culture, extruding cells were manually scored as non-apoptotic extruding, apoptotic extruding, or blocked apoptotic extrusions based on the presence of an actin ring and caspase-3 staining in 10,000 monolayer cells.

Statistical Analyses

Statistical analysis was done on at least four independent experiments for the overcrowding control and time analysis. Three separate assays were used for drug treatments and for FACS analysis. The error bars in all figures are the standard error of the mean (s.e.m.). All p-values were determined from a two-sided unpaired student's t-test using GraphPad Prism software.

Fluorescent Activated Cell Scanning (FACS) and proliferation analysis

Confluent homoeostatic, UV, and overcrowding monolayers were rinsed 3 times with PBS to remove any previous cells in suspension. The media was replaced and collected at each denoted analyses time. Media was collected and centrifuged at 3000 rpm in a Damon/IEC Division Clinical Centrifuge for 1 minute. The cells were resuspended in 250ul of PBS containing 4μg/ml propidium iodide and analysed by FACS. Samples were analysed on a Beckman Dickinson FACScan and 50–1000 cells were analysed for propidium iodide fluorescence at each condition. For proliferation analysis, pelleted cells were instead replated in a 96 well dish and representative pictures were taken at 24hrs and 5 days after replating. Results are from three independent experiments.

Zebrafish Care and Maintenance

Adult zebrafish were maintained under standard laboratory conditions, with a regular light/dark cycle of 14 hours light and 10 hours of darkness. Embryos were collected and raised in E3 embryo medium at 28.5 °C and staged according to[26]. The Institutional Animal Care and Use Committee (IACUC) at the University of Utah (Animal Welfare Assurance #10-07017) have approved all procedures performed in this protocol using the zebrafish, Danio rerio.

Zebrafish Drug Treatments

Zebrafish embryos were dechorionated at 24 hours post-fertilization (hpf). At 32 hpf approximately 50–100 embryos were transferred to dishes containing E3 embryo medium with or without (control) 10mM Gd^{3+} and allowed to develop at 28.5°C until 60 hpf, when the animals were either imaged live or fixed for immunostaining.

Zebrafish Immunostaining

Developing zebrafish larvae were fixed in 4% formaldehyde for 1–2 hours at room temperature or overnight at 4°C. Fixed specimens were then permeablised by rinses with PBSTx (0.5%) and incubated in blocking buffer (1% DMSO, 2mg/mL BSA, 0.5% Triton X-100 and 10% goat serum in PBS) for 2 hr. Specimens were then incubated overnight in primary antibodies for phospho-histone H3 (H3P, Abcam, 1:500) or activated caspase-3 (BD Pharmigen, 1:700). Samples were subsequently washed six times with PBSTx and then incubated in blocking buffer for 2hr before incubation with the appropriate secondary antibodies or Alexa-phalloidin (488/568/647) (Invitrogen). After incubation with secondary antibodies or Alexa-phalloidin, the specimens were rinsed five times with PBSTx, incubated with DAPI (1:1000) for 15 minutes, rinsed once more and then mounted in prolong gold. Depending on the situation, either whole specimens or only tail fragments (from the yolk extension back) were mounted for imaging. For quantification of H3P positive cells, the region from the cloaca back to the edge of the tail fin was quantified.

Zebrafish Imaging

Developing zebrafish were immunostained according to[6] and imaged with either the wide-field fluorescent microscope or a spinning disc confocal, described above. For live imaging, wild-type or Gd^{3+} treated developing *Tg(cldnb:lynGFP),* a kind gift from T. Piotrowski, zebrafish were anesthetised with 0.02% Tricaine in E3, mounted in 1% low melt agarose and imaged on a spinning disc confocal using a 20x objective, capturing a z-series every 2 minutes for 3–6 hours. Manual tracking of individual cells was performed using Metamorph.

Morpholino Antisense Oligonucleotide Knockdown of Piezo1

Developing zebrafish embryos were injected with 2–4ng of a standard translation blocking antisense morpholino oligonucleotides directed against the 5′UTR of *piezo1* (Accesssion# XM_691263) at the 1–2 cell stage and then allowed to develop at 28.5°C. For the photo-cleavable morpholino experiments, the translation blocking antisense morpholino (TBMO) was mixed at a 1:1 molar ratio with a sense-photo morpholino, with a 4bp mismatch around the photo-linker (see Supplementary Fig. 8c for schematic of strategy) and then injected into 1–2 cell stage wild-type AB or *Et(Gal4VP16)^{zc1044a};Tg(UAS-E1b:Kaede)^{s1999t}* embryos. At

28-32hpf, the developing embryos were then exposed to 350nm light for 20 seconds using a 10x objective on a Nikon 90i wide-field fluorescent microscope to activate the morpholino. Some injected embryos were not converted as a control for "leakiness" of the sense-photo MO. Likewise, some wild-type or Kaede expressing embryos that were not injected were exposed to 350nm light to ensure photo-conversion did not cause any adverse effects.

Morpholinos:

FAM38A 5′UTR TBMO: GAGCGACACTTCCACTCACATTCCT

FAM38A UTR pho 4m: AGGAATGTGAaaxttAGTGTCGCTC

Western Blot Analyses of Piezo1

piezo1 TBMO injected animals (n=15–20) were collected at 28hpf and homogenized in lysis buffer, boiled at 85°C for 5 minutes, spun down and the supernatant collected. A Bradford assay was performed to assess protein concentration. 10–15μg of protein was run out on a 3–8% Tris-Acetate gel at 150V for 1 hour. Detection was performed with an anti-Piezo1 antibody (Proteintech Cat#15939-1-AP) using standard ECL (enhanced chemiluminescence) methods. HC11, a mammary epithelial cell line, was used as a control for protein levels in mammalian tissues. Piezo1 proteins levels are presented relative to the α-tubulin loading control. Quantification of the scanned blot was performed using Image J.

Zebrafish embryos expressing the photoconvertable protein Kaede in the epidermis

To generate the *Et(Gal4VP16;myl7:GFP)*^{zc1044a} enhancer-trap line, a plasmid along with *tol2* mRNA was injected into 1-cell stage developing zebrafish embryos. The potential founders were then crossed to *Tg(UAS-E1b:Kaede)*^{s1999t} [28] and subsequently identified by Kaede expression. The identified F1 transgenic embryos were then imaged at 2 and 5 days post-fertilization for identification and characterization of epithelial specific expression patterns.

Supplementary Material

Refer to Web version on PubMed Central for supplementary material.

Acknowledgments

We thank Drs. Bryan Welm, Michael Redd, and Katherine Ullman for valuable input on our manuscript and Drs. Tom Marshall and Daniel Andrade for LifeAct and Bcl-2 expressing MDCK lines. The custom-design cell culture device was made with the support of National Institute of Biomedical Imaging and Bioengineering Grant EB-4443 to M. Yoshigi (patent pending). This work was supported by a NIH-NIGMS NIH Director's New Innovator Award 1 DP2 OD002056-01 and a Laura and Arthur Colwin Endowed Marine Biology Laboratories Summer Research Fellowship Fund to J.R. and a P30 CA042014 awarded to The Huntsman Cancer Institute for core facilities. An NIH Multidisciplinary Cancer Training Program Grant 5T32 CA03247-8 and American Cancer Society Salt Lake City Postdoctoral Fellowship (120464-PF-11-095-01 CSM) supported G.T.E., the University of Utah Undergraduate Research Opportunities Program Parent Fund Assistantship supported P.D.L, and an NIH R01 MH092256 supported H.O. and C.B.C.

References

1. Fan Y, Bergmann A. Apoptosis-induced compensatory proliferation. The Cell is dead. Long live the Cell! Trends Cell Biol. 2008; 18:467–73. [PubMed: 18774295]

2. Fan Y, Bergmann A. Distinct mechanisms of apoptosis-induced compensatory proliferation in proliferating and differentiating tissues in the Drosophila eye. Dev Cell. 2008; 14:399–410. [PubMed: 18331718]
3. Ryoo HD, Gorenc T, Steller H. Apoptotic cells can induce compensatory cell proliferation through the JNK and the Wingless signaling pathways. Dev Cell. 2004; 7:491–501. [PubMed: 15469838]
4. Rosenblatt J, Raff MC, Cramer LP. An epithelial cell destined for apoptosis signals its neighbors to extrude it by an actin- and myosin-dependent mechanism. Curr Biol. 2001; 11:1847–57. [PubMed: 11728307]
5. Gu Y, Forostyan T, Sabbadini R, Rosenblatt J. Epithelial cell extrusion requires the sphingosine-1-phosphate receptor 2 pathway. J Cell Biol. 2011; 193:667–76. [PubMed: 21555463]
6. Slattum G, McGee KM, Rosenblatt J. P115 RhoGEF and microtubules decide the direction apoptotic cells extrude from an epithelium. J Cell Biol. 2009; 186:693–702. [PubMed: 19720875]
7. Monks J, Smith-Steinhart C, Kruk ER, Fadok VA, Henson PM. Epithelial cells remove apoptotic epithelial cells during post-lactation involution of the mouse mammary gland. Biol Reprod. 2008; 78:586–94. [PubMed: 18057312]
8. Riedl J, et al. Lifeact: a versatile marker to visualize F-actin. Nat Methods. 2008; 5:605–7. [PubMed: 18536722]
9. Emoto Y. Cellular aggregation facilitates anoikis in MDCK cells. J Physiol Sci. 2008; 58:371–80. [PubMed: 18842164]
10. Gilmore AP. Anoikis. Cell Death Differ. 2005; 12 (Suppl 2):1473–7. [PubMed: 16247493]
11. Reddig PJ, Juliano RL. Clinging to life: cell to matrix adhesion and cell survival. Cancer Metastasis Rev. 2005; 24:425–39. [PubMed: 16258730]
12. Andrade D, Rosenblatt J. Apoptotic regulation of epithelial cellular extrusion. Apoptosis. 2011; 16:491–501. [PubMed: 21399977]
13. Tournier C, et al. Requirement of JNK for stress-induced activation of the cytochrome c-mediated death pathway. Science. 2000; 288:870–4. [PubMed: 10797012]
14. Coste B, et al. Piezo1 and Piezo2 are essential components of distinct mechanically activated cation channels. Science. 330:55–60. [PubMed: 20813920]
15. Olsen SM, Stover JD, Nagatomi J. Examining the role of mechanosensitive ion channels in pressure mechanotransduction in rat bladder urothelial cells. Ann Biomed Eng. 39:688–97. [PubMed: 21104316]
16. Bhattacharya MR, et al. Radial stretch reveals distinct populations of mechanosensitive mammalian somatosensory neurons. Proc Natl Acad Sci U S A. 2008; 105:20015–20. [PubMed: 19060212]
17. Yang XC, Sachs F. Block of stretch-activated ion channels in Xenopus oocytes by gadolinium and calcium ions. Science. 1989; 243:1068–71. [PubMed: 2466333]
18. Haas P, Gilmour D. Chemokine signaling mediates self-organizing tissue migration in the zebrafish lateral line. Dev Cell. 2006; 10:673–80. [PubMed: 16678780]
19. Tallafuss A, et al. Turning gene function ON and OFF using Sense- and Antisense-photo-Morpholinos in zebrafish. In press.
20. Holgate ST. The airway epithelium is central to the pathogenesis of asthma. Allergol Int. 2008; 57:1–10. [PubMed: 18209502]
21. Knight DA, Holgate ST. The airway epithelium: structural and functional properties in health and disease. Respirology. 2003; 8:432–46. [PubMed: 14708552]
22. Swindle EJ, Collins JE, Davies DE. Breakdown in epithelial barrier function in patients with asthma: identification of novel therapeutic approaches. J Allergy Clin Immunol. 2009; 124:23–34. quiz 35–6. [PubMed: 19560576]
23. Shraiman BI. Mechanical feedback as a possible regulator of tissue growth. Proc Natl Acad Sci U S A. 2005; 102:3318–23. [PubMed: 15728365]
24. Yoshigi M, Clark EB, Yost HJ. Quantification of stretch-induced cytoskeletal remodeling in vascular endothelial cells by image processing. Cytometry A. 2003; 55:109–18. [PubMed: 14505316]

25. Yoshigi M, Hoffman LM, Jensen CC, Yost HJ, Beckerle MC. Mechanical force mobilizes zyxin from focal adhesions to actin filaments and regulates cytoskeletal reinforcement. J Cell Biol. 2005; 171:209–15. [PubMed: 16247023]

26. Kimmel CB, Ballard WW, Kimmel SR, Ullmann B, Schilling TF. Stages of embryonic development of the zebrafish. Dev Dyn. 1995; 203:253–310. [PubMed: 8589427]

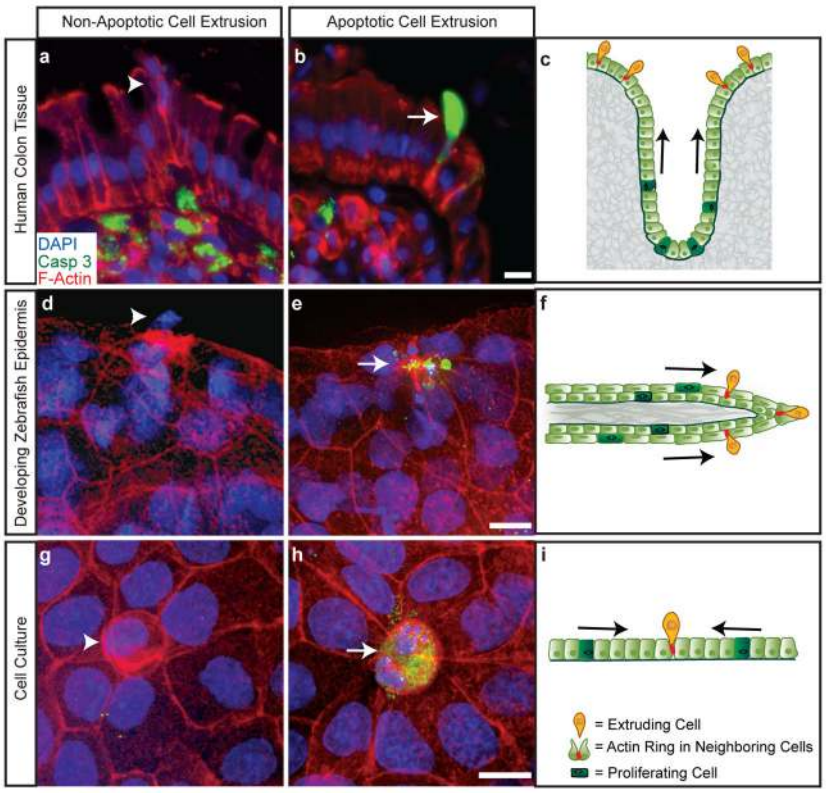

Figure 1. Both apoptotic and non-apoptotic epithelial cells extrude at locations of high crowding during homeostasis and development

Non-apoptotic (caspase-negative) and apoptotic (caspase-positive) extrusions at the surface of human colon epithelia (**a, b**), zebrafish epidermis (**d, e**), and confluent MDCK monolayers (**g, h**). Extrusions typically occur at sites of high crowding (indicated by yellow cells in **c, f, and i**). Arrows indicate direction of force from mitoses and migration. Scale bars=10 μm.

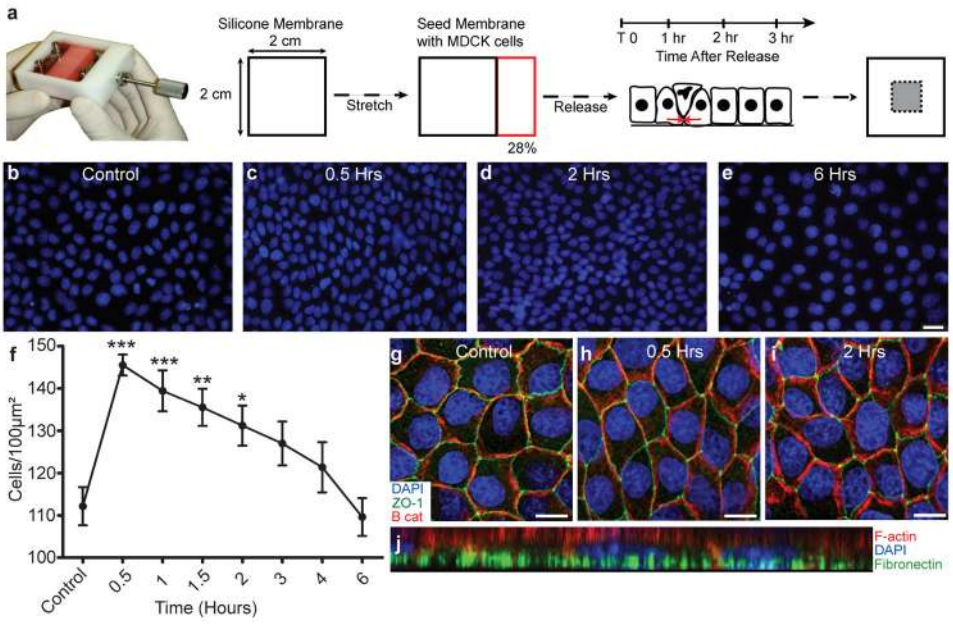

Figure 2. Characterisation of experimental overcrowding

(**a**), Experimental design for overcrowding monolayers grown on stretched matrix. Only cells in the grey area (right) were analysed to ensure a homogeneous strain field. (**b–e**) Images of the nuclei of control unstretched monolayers, and monolayers 0.5–6 hours post-overcrowding were quantified in (**f**). Mean number of nuclei per field is plotted, error bars represent s.e.m. (**g–i**) Monolayers at 0.5 and 2 hours post-release show that adherens and tight junctions maintain integrity after overcrowding, as compared to control. (**j**), Monolayer stained for actin and DNA at 2 hours after release on Cy5-labeled fibronectin shows that contacts to substratum are maintained. Scale bars = 10 μm. ***=p<0.0005, **=p<0.005, *=p<0.05.

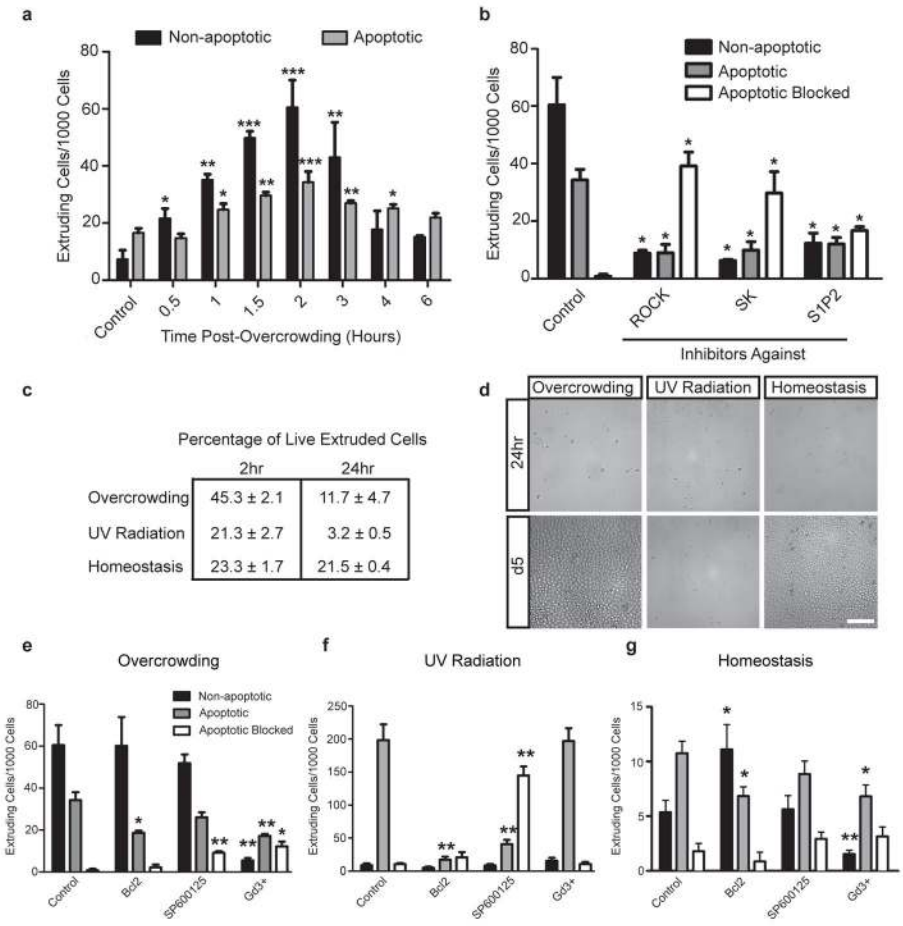

Figure 3. Overcrowding MDCK monolayers promotes extrusion of non-apoptotic cells

(a), Quantification of live and apoptotic extruding cells 2 hrs post-overcrowding. (**b**), Live cell extrusion requires ROCK, Sphingosine Kinase, and $S1P_2$ (JTE-013). (**c**), Cell viability 2 or 24 hrs after extrusion. (**d**), Growth of extruded cells collected at 2 hrs post crowding after 24hrs and 5 days. Gd^{3+} inhibits both overcrowding-induced extrusion (**e**) and homeostatic extrusion (**g**) whereas Bcl-2 over-expression and JNK inhibition only affect UV-C-induced apoptotic extrusion (**f**). n ≤7 independent experiments, mean ± s.e.m. Scale bars=100 μm. ***=p<0.0005, **=p<0.005, *=p<0.05.

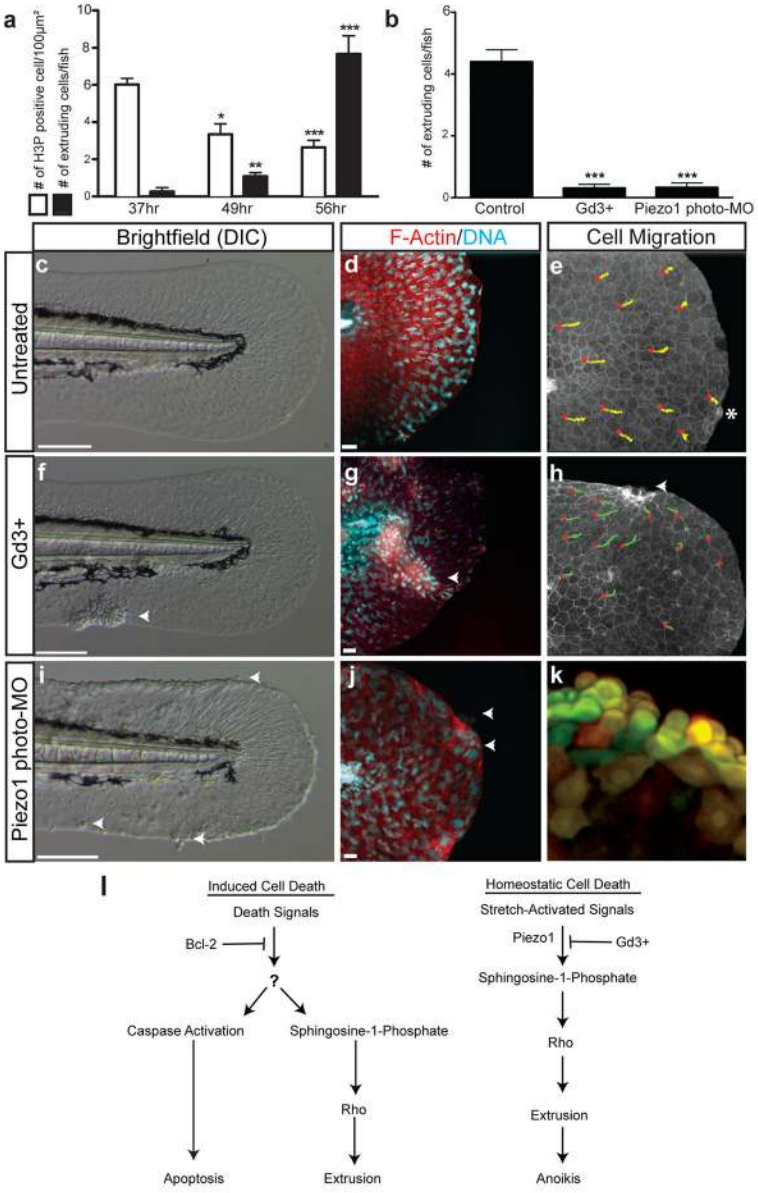

Figure 4. Disrupting the stretch-activated channel Piezo1 *in vivo* blocks live cell extrusion and causes epithelial mass formation

(**a**) Proliferation and extrusion rates during zebrafish tail fin development. (**b**) Gd^{3+}-treatment and *piezo1* photo-MO block extrusion (n=15–17 embryos from 3 independent experiments, mean ± s.e.m). Brightfield and confocal projections of untreated (**c,d**), Gd^{3+}-treated (**f,g**), and *piezo1* photo-MO knockdown (**i, j**) in 60hpf developing zebrafish. (**e, h**), Tracks from red circle mark the movement of individual epithelial cells in control and Gd^{3+}-treated *Tg(cldnb:lynGFP)* developing zebrafish. (**k**) Epidermal cell mass from a *piezo1* photo-MO knockdown in Kaede zebrafish, where yellow cells are photo-converted. (**l**), Model of induced cell death versus homeostatic cell death. Arrowheads denote cell

accumulations and asterisk an extrusion. Scale bars in **c, f, & i** = 100 μm, in **d, g, & j** =10 μm. ***=p<0.0005, **=p<0.005, *=p<0.05.